Generation of Hydrophilic, Bamboo-Shaped Multiwalled Carbon Nanotubes by Solid-State Pyrolysis and Its Electrochemical Studies

Sangaraju Shanmugam and Aharon Gedanken*

Department of Chemistry and Kanbar Laboratory for Nanomaterials at the Bar-Ilan University Center for Advanced Materials and Nanotechnology, Bar-Ilan University, Ramat-Gan, 52900, Israel

Received: October 9, 2005; In Final Form: December 8, 2005

A simple, efficient, and novel method was developed for the direct preparation of hydrophilic, bamboo-shaped carbon nanotubes by the pyrolysis of ruthenium(III) acetylacetonate in a Swagelock cell is reported. The obtained product exhibits mostly bamboo-shaped, straight, periodic twisted, multiwalled carbon nanotubes possessing diameters of 50−80 nm and lengths of around 10 μm. The pyrolyzed product was characterized by scanning electron microscopy (SEM), transmission electron microscopy (TEM), high resolution TEM (HRTEM), Fourier transform infrared (FT-IR), X-ray photoelectron spectroscopy (XPS), micro-Raman, and cyclic voltammetric techniques. HRTEM studies showed that the walls of bamboo-shaped carbon nanotubes consisted of oblique grapheme planes with respect to the tube axis. The interlayer spacing between two graphitic layers was found to be 0.342 nm. XPS measurements have suggested that as-prepared carbon nanotubes consist the surface functional groups on the surface of carbon nanotubes. The electrochemical properties of synthesized carbon nanotubes have been evaluated. Thermogravimetric analysis (TGA), IR, and cyclic voltammetric studies showed the presence of oxygen functionalities. Raman studies revealed the presence of disorder in the graphitic carbon and the presence of exposed edge plane defects in the generated carbon nanotubes for influencing the surface behavior and electrochemical properties. The electrochemical behavior of electrodes made of bamboo-shaped carbon nanotubes served for an oxygen reduction reaction.

Introduction

Carbon nanotubes (CNTs) have attracted much attention because of their unique structural, electronic, magnetic, and mechanical properties.[1] There are numerous synthetic procedures for the preparation of carbon nanotubes such as arc-discharge,[2−4] laser ablation,[5] and chemical vapor deposition (CVD)[6] of various molecules over metallic catalysts. Among the available synthetic methods for their preparation, chemical vapor deposition has emerged as the most effective. In CVD, if no catalyst is used, amorphous carbon is mainly produced. The catalyst required for CVD can be pure metals, metal salts, or organometallic complexes. The introduction of the floating catalyst process by Qin was an important step in the synthesis of multiwalled nanotubes (MWNTs).[7] A metal catalyst is continuously supplied to the gas phase instead of being supported on the substrate. This allows a high throughput growth of multiwalled carbon nanotubes (MWCNTs). For this purpose, various precursors have been employed such as metal carbonyls, metallocenes, and metallophthalocyaninces. The catalytic decomposition of hydrocarbons is a promising route to produce carbon nanotubes in large quantities.[8] Recently, Iyer et al. adopted a single component approach to the fabrication of MWCNTs in the pyrolysis of a suitable organometallic precursor and obtained near-quantitative yields.[9] Wu et al. obtained a mixture of bamboo-shaped and straight carbon nanotubes by the theromolysis of hexa-peri-hexabenzonocoronene−cobalt complexes.[10] Thus, the choice of the preparation method and the metal precursor is important for obtaining the desired type of carbon nanotubes. Recently, much attention was paid to the shape and morphology of carbon nanotubes. Bamboo-,[11] octopus-[12] and herringbone-shapes[13] were obtained, structures that are different from conventional nanotubes. The bamboo-shaped MWNTs were prepared by various methods such as arc-evaporation, chemical vapor deposition, and the pyrolysis of various organometallic precursors.

Carbon nanotubes have been employed as catalyst supports for various purposes such as fuel cell and liquid phase reactions.[14] To support the active entities over the carbon nanostructures, they should possess some functional groups to anchor or to hook up the active entities on the functional groups. However, unfortunately, the carbon nanotubes generated by the chemical vapor deposition method are hydrophobic, and so, introducing the functional groups required special methods.[15−19] Treatment of carbon nanotubes with existing oxidizing agents in the gas or liquid phase results in the formation of oxidic groups such as carboxy, carboxylic anhydride, lactone, phenolic, carbonyl, and quinone groups on the skeleton of the carbon nanotubes. To use carbon nanotube materials for electrochemical applications involving aqueous electrolytes, the carbon nanotube-based electrode needs to be pretreated so that it is easily wetted when immersed in the solution.[20] Various electrochemical oxidation methods have been proposed to effectively introduce oxygen functionalities.[21] By adopting harsh electrochemical methods, either the longer tubes broke down into smaller tubes or fracture of the carbon nanostructures was observed.[22] Wang reported carbon encapsulated palladium by the arc method.[23] Metal encapsulated or filled MWCNTs were prepared by Liu et al.[24] Recently, Geng et al. synthesized carbon nanotubes or Ni nanoparticles encapsulated in graphitic cages by pyrolysis of nickel stearate in argon atmosphere.[25]

Various transition metal catalysts have been employed for the synthesis of CNTs, such as iron,[26] cobalt,[27] nickel,[28] copper,[29]

* E-mail: gedanken@mail.biu.ac.il.

10.1021/jp055749g CCC: $33.50
Published on Web 01/13/2006

molybdenum,[30] rhodium,[31] palladium,[32] and gold.[33] The number of papers reporting on the involvement of Ru as a catalyst in the synthesis of CNT is very limited. One of these papers uses a supported metallic-ruthenium catalyst,[34] while another paper describes the employment of ruthocene and ferrocene dissolved in xylene. This mixture was continuously fed to a preheated chamber. The resulting vapor was employed for the fabrication of Ru-doped CNTs by the CVD method.[35] There is no report on the direct ruthenium-catalyzed synthesis of CNTs.

A second novelty of the current paper is related to the hydrophilic nature of the Ru−CNT surface. Usually, the CNTs or carbon nanofibers (CNFs) prepared by the CVD method are mostly hydrophobic in nature.[36] This makes the synthesized Ru−CNT unique and useful for electrochemical applications. Herein, we report a simple, efficient method for the preparation of bamboo-shaped carbon nanotubes. The direct pyrolysis of ruthenium(III) acetylacetonate was carried out at 1000 °C for stipulated time periods. The product was characterized by SEM, TEM, HRTEM, IR, XPS, and micro-Raman techniques. HRTEM and XRD results showed the presence of metallic ruthenium nanoparticles in the carbon nanotubes. The obtained carbon nanotubes are of a hydrophilic nature, which is evidenced from IR spectroscopy, from cyclic voltammetry, and also from wetting analysis. The electrochemical studies were carried out in an acidic aqueous solution. Preliminary studies of bamboo-shaped, carbon nanotube electrodes prepared from the pyrolysis of ruthenium(III) acetylacetonate demonstrated a high electrocatalytic activity for oxygen reduction in 1 M sulfuric acid.

Experimental Section

The ruthenium(III) acetylacetonate was obtained from Aldrich. All other compounds were of reagent grade and used as received. The synthesis of bamboo-shaped carbon nanotubes was carried out using a Swagelok union cell, which was assembled from stainless steel Swagelok parts. A $^3/_4$ in. union part was plugged from both sides by standard caps. For this synthesis, 0.5 g of ruthenium acetylacetonate was introduced into the cell at room temperature under atmospheric conditions. The filled cell was closed tightly with the other plug and then placed inside an iron pipe at the center of the furnace. The temperature was raised at a heating rate of 20 °C per minute. The closed vessel cell was heated at 1000 °C for 10h. The reaction took place under the autogenic pressure of the precursor. The closed vessel cell (Swagelok) heated to 1000 °C was gradually cooled to room temperature and opened with the release of a little pressure. The total weight of products determined gravimetrically was 0.325 g of black powder, which constitutes 65% mass recovery.

Structural Characterization. Scanning electron microscopy (SEM) of the obtained product was carried out on a JEOL-JSM 840 scanning electron microscope operating at 10 kV. The particle morphology was studied with transmission electron microscopy (TEM) on a JEOL-JEM 100 SX microscope, working at an 80 kV accelerating voltage, and on a JEOL-2010 high resolution TEM (HRTEM) instrument with an accelerating voltage of 200 kV. Samples for TEM and HRTEM were prepared by ultrasonically dispersing the products into absolute ethanol, then placing a drop of this suspension onto a copper grid coated with an amorphous carbon film, and then drying under air. The elemental analysis of the sample was carried out using an Eager C, H, N, S analyzer. An Olympus BX41 (Jobin Yvon Horiba) Raman spectrometer was employed, using the 514.5 nm line of an Ar laser as the excitation source to analyze the nature of the carbon present in the products. X-ray photoelectron spectroscopy (XPS) measurements were performed in ultrahigh vacuum (UHV) with Kratos, axis HS monochromatized Al Kα cathode source, at 75−150 W, using a low energy electron plod gun for charge neutralization. Survey and high resolution individual metal emissions were taken at a medium resolution, with a pass energy of 80 eV and a step of 50 meV.

Electrochemical Characterization. A single glass compartment, three-electrode cell was employed for the cyclic voltammetry and chronoamperometry studies. Pt wire and saturated calomel electrodes (SCE) were used as counter and reference electrodes, respectively. A 0.076 cm^2 area glass carbon (GC) served as the working electrode. The electrochemical studies were carried with a potentiostat/galvanostat model 273 A. A 10 mg portion of bamboo-shaped carbon nanotubes were dispersed in 0.5 mL of water for 20 min in an ultrasonicator. The dispersed carbon nanotubes (10 μL) were placed on GC and dried in an oven at 90 °C for 2 min. A 5 μL portion of 5% Nafion was dropped on GC and dried at room temperature. The solvent was evaporated, and the Nafion acted as a binder to the hold the carbon nanotubes to the electrode. For the electrochemical oxygen reduction, the electrolyte was saturated by purging with oxygen gas. The electrolyte was degassed with nitrogen gas before the electrochemical measurements.

Results and Discussion

The SEM micrograph of the obtained product is shown in Figure 1a. The micrograph shows swirled carbon nanotubes and no other amorphous carbon or other graphitic carbon nanostructures. The low resolution TEM of the product shows mostly bamboo-shaped carbon nanotubes (80%), straight carbon nanotubes, and a few twisted carbon nanotubes (Figure 1b). Similarly to the SEM, no carbon particles are detected in the TEM picture. The twists are seen periodically in the carbon nanotubes and are shown by an arrow in Figure 1b. The width of the twisted flat part is around 17 nm with a length of about 300 nm. The bamboo-shaped carbon nanotubes are mostly present in a swirled form. A representative snakelike, bamboo-shaped carbon nanotube is presented in Figure 1c. From Figure 1b, it is clear that the size of the carbon nanotubes having a bamboo-shaped structure is about 30−50 nm in diameter with a length of several micrometers.

Figure 2a shows the bamboo-shaped nanotubes with an open end and also a twisted carbon nanotube. The dotted arrow indicates the start of a twist. The length of the twist is around 300 nm, shown in Figure 2a. We observed periodic twists in the twisted carbon nanotubes. The distance between two twists is around 1100 nm. The diameter of a twist is around 17 nm and consists of around 48 graphic layers.[37] The carbon nanotubes have been converted to carbon nanosheets in order to minimize the torsional force in the tubular structure. Some of the nanosheets contained periodic twists. The bamboo-shaped carbon nanotubes are comprised of an outer diameter of about 50−85 nm and an inner diameter of about 25−35 nm. The bamboo-shaped carbon tube is made up of several compartments of almost uniform size. Most of the compartments were empty, while a few contained ruthenium metal nanoparticles present at the end of the compartments. Figure 2b also shows defective graphitic layers which arise because of the release of the strain present in the carbon nanotube. Two individual bamboo-shaped CNTs formed in two different direction growths are represented in Figure 2c. The dark arrows indicate the direction of the bamboo-shaped compartment in the carbon nanotubes. The arrow shown in the micrograph reveals that the formation

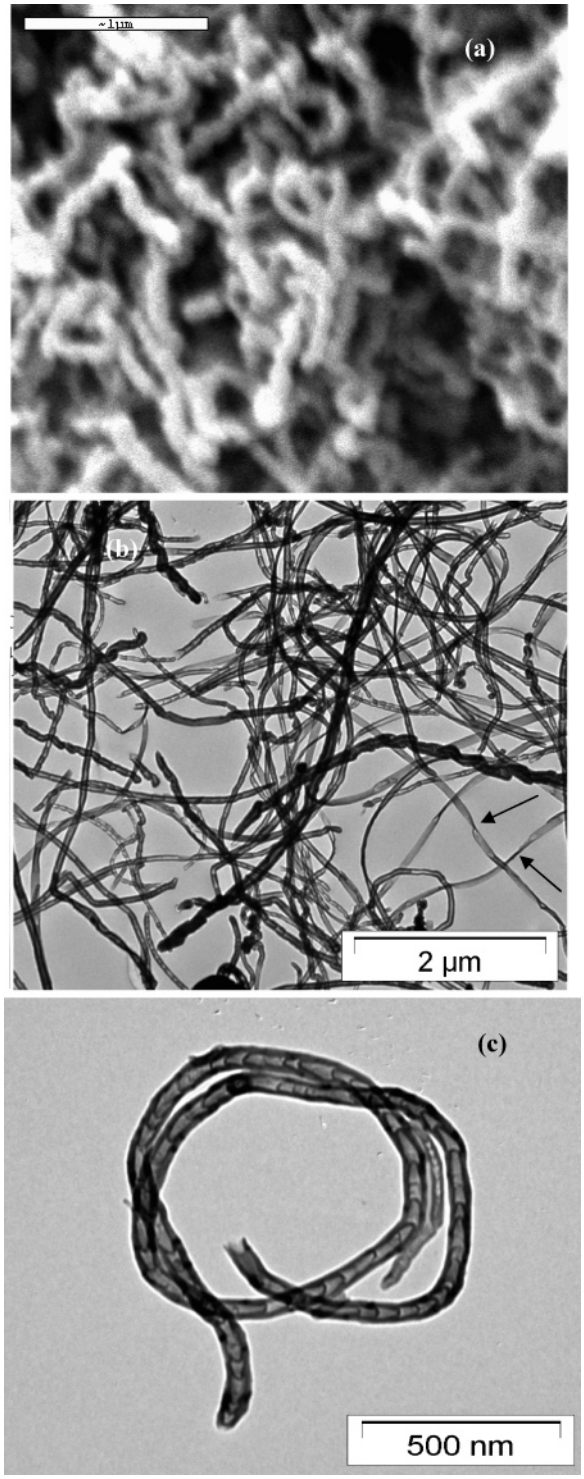

Figure 1. (a) Representative SEM image of carbon nanotubes, (b) TEM image showing existence of bamboo-shaped, straight, and twisted MWCNTs (arrows shows twists in carbon nanotubes), and (c) an individual bamboo-shaped snake-like carbon nanotube.

of the compartment initiates from the wall of the previous compartment. This is the first such type of bamboo-shaped growth in the carbon nanotubes. The size of the compartments is around 200 nm in most of the bamboo-shaped CNTs. We also observed a few graphitic subcompartments in the main compartments, which can be visualized from Figure 2c. The compartments of the bamboo structure also possessed graphitic layers (normally 30−45 layers in the wall and 5−10 layers in the middle wall). Figure 2d presents the HRTEM image of a bamboo-shaped CNT showing the wall and compartmentalized graphitic layers. The two graphitic planes were separated by a distance of 0.342 nm, which is almost like that in ordinary CNTs. It should be noted that the graphitic layers are not arranged in parallel to the axis of the tube. The wall has herringbone graphitic layers. The wall thickness is around 12 nm, becoming as thin as 9 nm at the joint and, then, returning to a thickness of 12 nm after the joint. It can be seen from the micrograph that there is a dangling graphitic layer (see arrow 2) with a thickness of 10 nm, while, beneath that, there is another graphitic wall which continued the growth of another compartment. The graphitic layers grown were conical in shape. Figure 3 shows the HRTEM image of a carbon nanotube containing the spherical metallic nanoparticles at the tip of the tubes. HRTEM revealed that the interlayer spacing of a metal nanoparticle is about 0.212 nm, consistent with the (002) plane of metallic hexagonal Ru (see the Supporting Information, SI-3). The presence of ruthenium nanoparticles was also confirmed from XRD analysis (see the Supporting Information, SI-2). The diffraction of the peak (at 26.5°) is due to graphitic (002) reflections. The other peaks are well indexed to a typical hexagonal phase of Ru. The ruthenium nanoparticles are present at the end of the bamboo compartments. The HRTEM image of the graphitic shells at the right upper part of Figure 3b was well resolved. We proposed the growth of bamboo-shaped carbon nanotubes in terms of surface and bulk diffusion of carbon based on a mechanism proposed in the literature.[38] The carbon atoms, which are produced via pyrolysis of ruthenium acetylacetonate impinging on metal nanoparticles, form a cap to the metal nanoparticle. If carbon is continuously supplied, they diffuse through the metal nanoparticle due to the gradient in the carbon density within the nanoparticle. Once the formation of the graphitic sheet starts, the diffusion of carbons accelerates into the reaction zone of the catalytic particle, thus the carbons are continuously added to the edge of cap. The hollow and bamboo-shaped carbon nanotubes were formed on different sizes of metal nanoparticles. We also anticipated similar effects in our method. For smaller nanoparticles, surface diffusion of carbon gave rise to CNT walls, while, for the surface diffusion and bulk diffusion of larger metal particles, both processes are the source of wall formation. Bulk diffusion is the main source for the growth of the internal structures in characteristic bamboo-shaped CNTs.

The Raman spectra of bamboo-shaped carbon nanotubes were recorded to assess the relative amount of basal and edge plane graphitic carbon. Figure 6 shows the Raman spectra of carbon nanotubes indicating the presence of two strong peaks at 1346 and 1575 cm^{-1}, commonly known as the D and G bands of carbon nanotubes. The inset of Figure 6 shows the breathing modes of bamboo-shaped carbon nanotubes. The peak at 1575 cm^{-1} corresponds to an E_{2g} mode of graphite, which is due to the sp^2-bonded carbon atoms in a two-dimensional hexagonal graphitic layer.[39] The D band at around 1346 cm^{-1} is associated with the presence of defects in the hexagonal graphitic layers. The ratio of the intensities of the D and G bands is known to be correlated to the quality of the carbon nanotubes, which is used to estimate the degree of disorder in the graphic carbon. An I_D/I_G ratio near zero indicates high crystallinity, and a value near 1 indicates the highly disordered nature of carbon nanotubes. The I_D/I_G ratio for the bamboo-shaped CNTs was found to be 0.520, suggesting that the CNTs are disordered and that significant edge plane sites exist.

Various properties of carbon materials, in particular their wetting and adsorption behavior, are decisively influenced by surface functional groups.[40] Oxygen on the surface of carbon

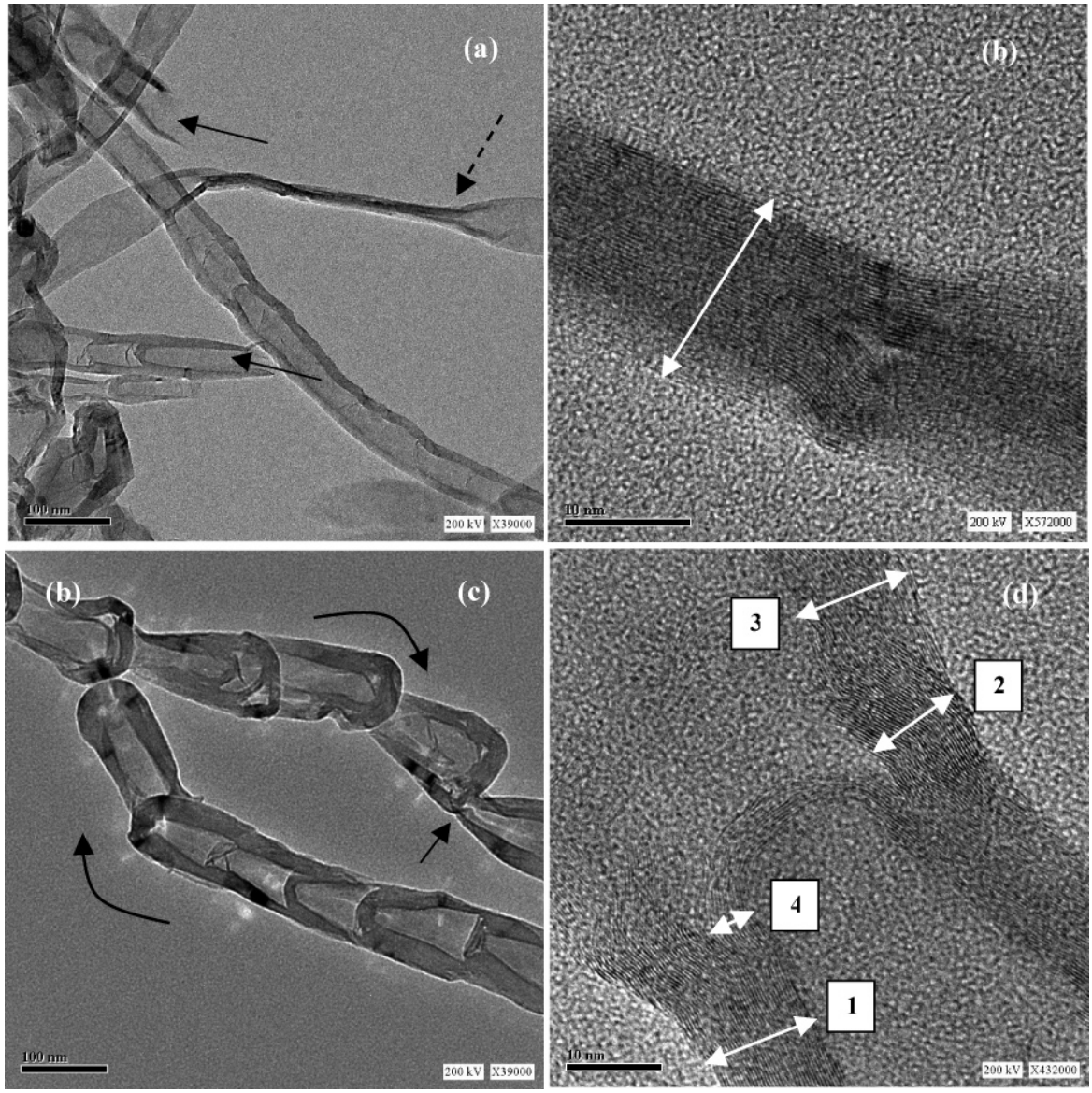

Figure 2. TEM images of the carbon nanotubes: (a) open bamboo-shaped carbon nanotubes (continuous arrow) and a twist in carbon nanotube (dotted arrow); (b) HRTEM image of resolved graphic fringes at the twisted area marked with a dotted arrow in part a; (c) bamboo-shaped CNTs with two different growth directions; (d) HRTEM image of a bamboo-shaped MWCNT, showing wall graphitic layers (see 1) and dangling graphitic layers (see 2) and, after compartmentalization, the original graphitic layers (see 3) and the compartment graphitic layers (see 4).

can exist in the form of various functional groups such as carboxy, carboxylic anhydride, lactone, phenolic, carbonyl, and quinone groups.[41] The surface of such carbons is heterogeneous. The carbon nanotube consists of the faces of a graphite plane with the basal plane, and the edge plane, perpendicular to the basal plane. The edge-plane sites are much more reactive than the graphite basal planes.[42]

We have carried out the thermal analysis of bamboo-shaped CNTs under N_2 atmosphere. The theromogravemetric analysis indicated that the weight loss in the region of 50−150 °C is due to the loss of water. Another weight loss of 2% was observed at the 150−450 °C range and is interpreted as due to the CO_2 released from the functional groups present on the carbon nanotubes (see the Supporting Information, SI-1). Our interpretation is based on Ros et al., who observed an ∼3% weight loss for the acid-(HNO_3/H_2SO_4) treated carbon nanotubes.[43] Ros et al. have analyzed the released gases and found CO_2 to be the main product in the 150−450 °C range. From the TGA analysis and the release of CO_2, it is clear that the as-prepared carbon nanotubes exhibit some oxygen surface functional groups such as carboxylic acid, lactones, or phenolic functional groups. The presence of oxygen-containing surface functional groups on carbon nanotubes was also established by IR spectroscopy. Infrared analysis shows the presence of the band at 1715 cm^{-1}, associated with >C═O in carboxyls or carboxylic anhydrides, and a broad band centered around 1221 cm^{-1}, associated with C—O stretching in ethers, phenols, carboxyls, and carboxylic anhydrides[43] (Figure 4). We have also carried out XPS measurements to see the surface functional groups on as-prepared bamboo-shaped MWCNTs. We observed an asymmetric peak centered at 285 ± 0.2 eV. We deconvolute the C_{1s} spectrum of MWCNTs into two symmetric peaks (285.0 ± 0.2 eV, 285.6 ± 0.2 eV) and an asymmetric peak (286.4 ± 0.2 eV) (Figure 5). The main peak (285 eV) originates from the graphitic carbon sp^2, from C—C and C—H forms of graphitic carbon. The peaks at 285. 6 and 286.4 can be assigned to sp^3-hybridized carbon atoms boned with one or two oxygen atoms, respectively. When the electronegative oxygen atoms are bonded to the carbon, a positive charge is induced on the carbon atom. Hence, they can be assigned to alcoholic, ether (C—O) and

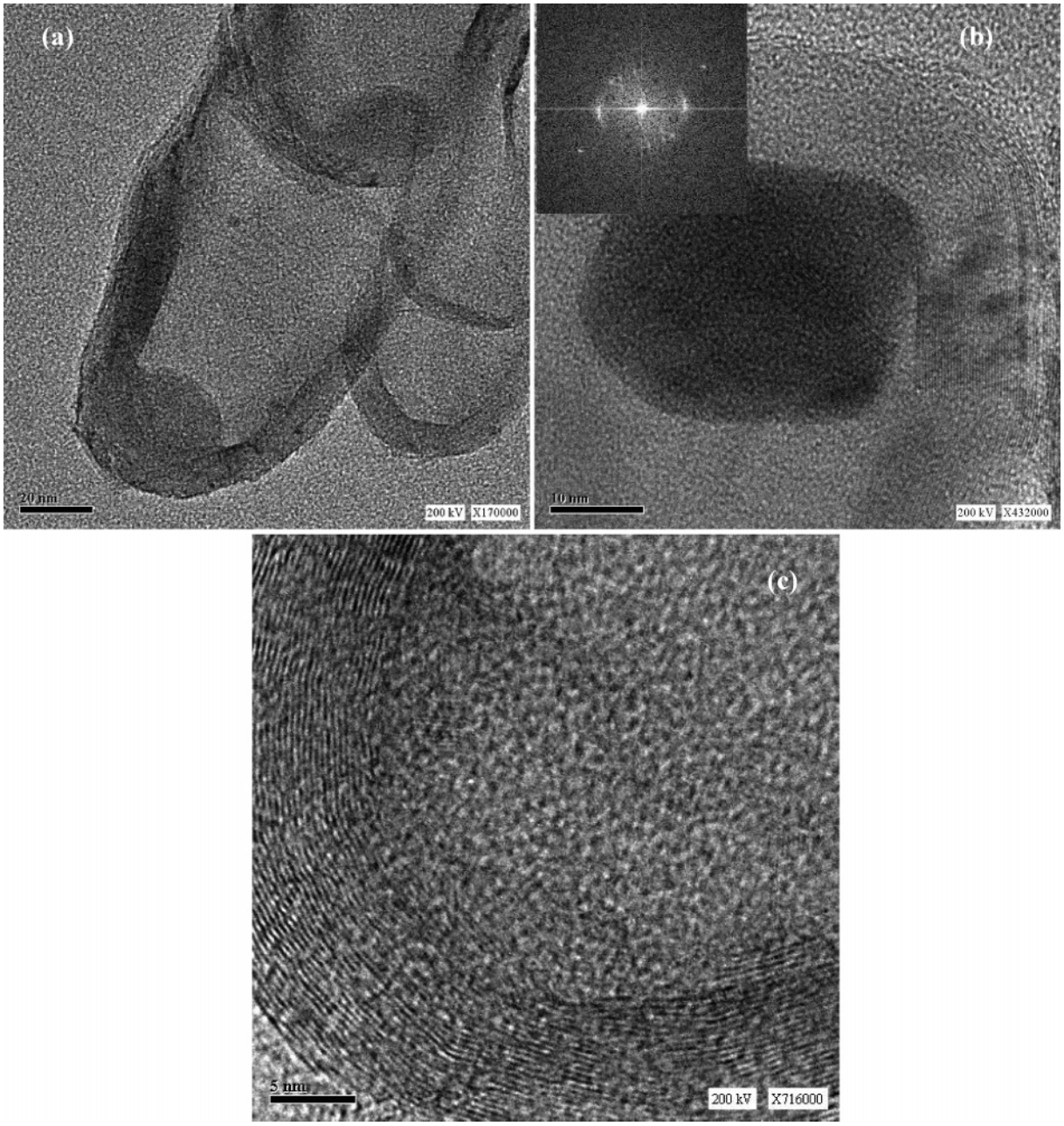

Figure 3. (a) TEM image of a metal nanoparticle embedded bamboo-shaped MWCNT, showing bisection into two nanotubes. (b) HRTEM image of a metal nanoparticle present in the tip of a carbon nanotube. The inset shows the fast Fourier transform (FFT) which corresponds to the ruthenium (002) and graphitic (002) planes. (c) HRTEM image of showing lattice fringes of the wall of a bamboo-shaped carbon nanotube.

ketone, aldehyde (>C═O) species.[44] It is clear from TGA, IR, XPS analysis, and cyclic voltammetry (CV) studies, that the as-prepared CNT has some oxygen functional groups on its surface. To further corroborate this behavior of bamboo-shaped CNTs, we have roughly assessed the nature of the surface of carbon nanotubes by dispersing ultrasonically 1 mg of carbon nanotubes in hexane/water (1/1) mixture for 30 min.[43,45] From our study, we observed that the carbon nanotubes were dispersed in a water layer (bottom), indicating the hydrophilic nature of the obtained bamboo-shaped carbon nanotubes.

Most of the electrochemical studies on carbon nanotubes were carried out with SWNTs due to their unique molecular structures. However, multiwalled carbon nanotubes (MWNTs) are potentially more attractive electrode materials because of their easy preparation and low cost.[46] Generally, MWNTs have larger diameters and better accessibility to the electrolytes and electrical conductivity than SWNTs. Other studies indicate that MWNTs have a fast electron transfer rate for various redox reactions. Campbell et al. demonstrated that a single multiwalled carbon nanotube electrode (200 nm in diameter) presents an ideal steady-state radial diffusion feature.[47]

The electrochemical characterization of the bamboo-shaped CNT is carried out in an acidic aqueous electrolyte without any redox probe in order to investigate oxygen functionalities. Figure 7 shows the cyclic voltammograms of a carbon nanotube electrode and a bare GC electrode in 1 M H_2SO_4. The carbon nanotube electrode exhibits an anodic peak at 447 mV and a cathodic peak at 395 mV. These peaks are due to protonation/deprotonation of surface functional groups (such as quinone/hydroquinone).[48,49] Recently, Kaempgen et al. observed a featureless cyclic voltammogram for a MWCNT-based microelectrode bundle in an aqueous electrolyte. They reported that no oxygen functional groups were present and that the MWCNTs synthesized by CVD are hydrophobic in nature.[50] The back-

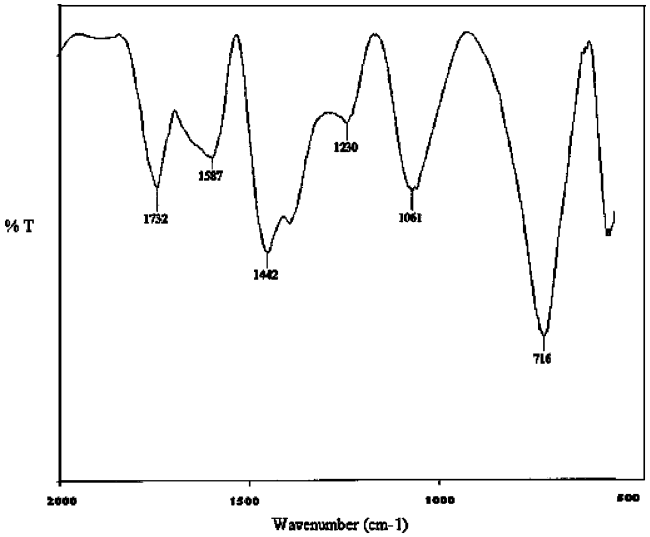

Figure 4. IR spectra of bamboo-shaped multiwalled carbon nanotubes.

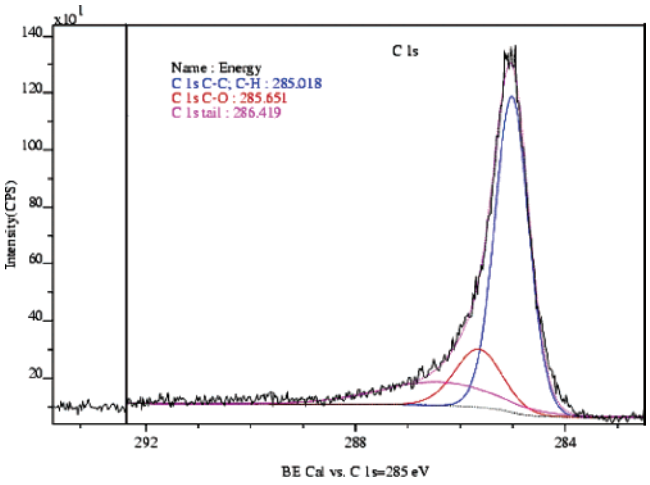

Figure 5. X-ray photoelectron spectra of C_{1s} of as-prepared bamboo-shaped MWCNTs.

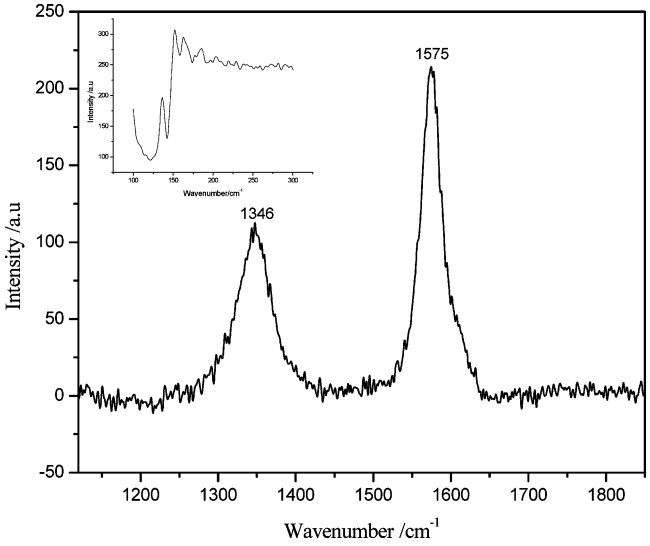

Figure 6. First-order Raman spectrum of MWCNTs showing the presence of disorder graphitic carbon

ground current for a carbon nanotube electrode is very much greater than that of a glassy carbon electrode (Figure 7). The high current response may be due to more exposure of graphic layer edge planes in bamboo-shaped nanotubes. In addition, the

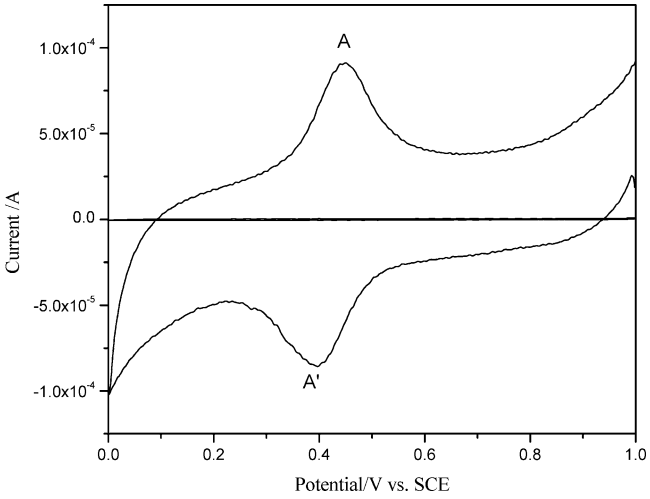

Figure 7. Cyclic voltammetric response of a bamboo-shaped carbon nanotube electrode (solid line) and a GC electrode (horizontal line) immersed in 1 M sulfuric acid. The scan rate is 25 mV/s.

inner surfaces of nanotubes are also accessible for the electrolyte. In bamboo-shaped carbon nanotubes, a high percentage of graphitic layers must terminate at the surface of tube, giving rise to a large number of edge plane or edge plane-like defect sites along the surface of the tube.[42] This higher electrochemically active surface area is a great advantage for electrochemical applications. The observed $E_{1/2}$ is assigned to the functional groups present in carbon nanotubes (quinone/hydroquinone). A similar electrochemical response was observed for the electrochemically oxidized carbon nanotubes.[49] In the present study, we observed a well-resolved peak in CV for oxygen functional groups for bamboo-shaped CNTs. To explain that the redox couple is originating from the surface functional groups of the MWCNT and not from the Ru metal, we have carried out CV measurements of Ru/TiO_2 under similar experimental conditions. We did not observe any redox peaks in the potential region. This study demonstrates that the redox peaks observed in our study are originating from the oxidation/reduction of surface quinodal functional groups from bamboo-shaped CNTs. The hydrophilic behavior of the bamboo-like nanotubes is the result of a significant amount of edges (or disorder) of graphitic carbon on the surface of bamboo-shaped CNTs. The cathodic-to-anodic peak current ratio is equal to 1, indicating a chemically reversible system.[51] The variation of the scan rate was carried out in order to understand the electrochemical process phenomenon. As the scan rate increases from 5 to 40 mV, the anodic peak is shifted to a more positive potential and cathodic peak is shifted to a negative potential (Figure 8a). A plot of the cathodic and anodic peak current vs the scan rate is linear, which is a characteristic of a surface-confined process (Figure 8b). The linearity of the plot indicates that the process is not diffusion-controlled in the studied scan rate. This plot also indicates the number of electrons which are involved, i.e, dividing the slope of the line with the area under the voltammogram at any scan rate is equal to $nF/4RT$, which showed one electron transfer. The origin of the redox peaks may be due to the oxidation/reduction of surface functional groups.[49] Ye et al. recently studied the capacitance behavior of electrochemically treated and untreated MWCNTs, and they observed that the electrochemically oxidized MWCNTs showed an 11 times higher capacitance than the untreated MWCNTs. The enhancement in the capacitance is due to the opening of the ends of CNTs or hydrophilic−hydrophobic properties of electrochemically oxidized MWCNTs.[49]

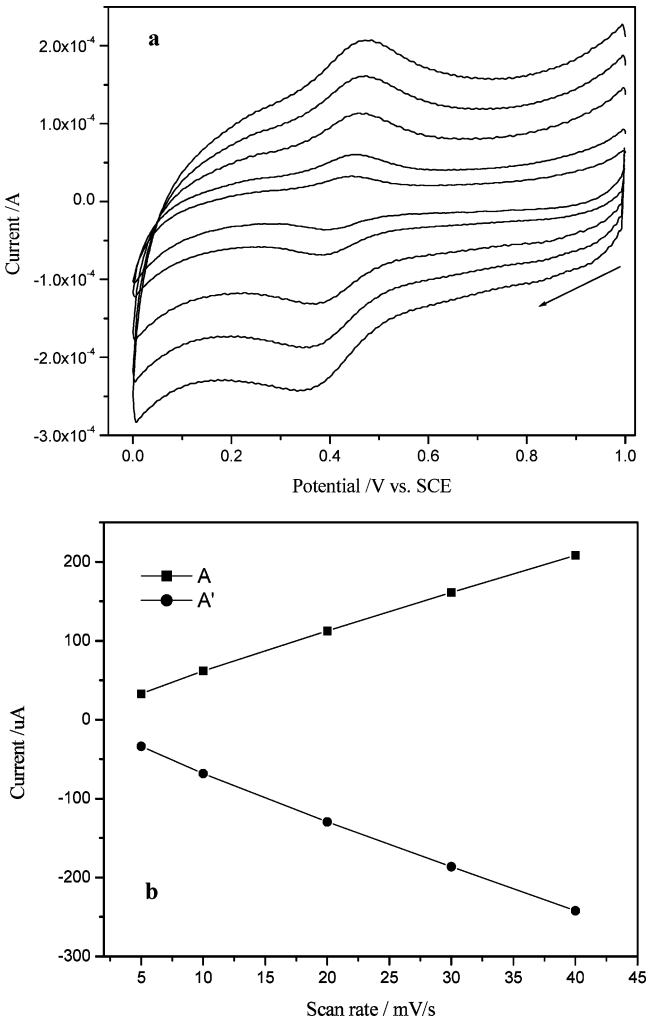

Figure 8. (a) Cyclic voltammograms of bamboo-shaped carbon nanotubes on GC in 1 M sulfuric acid. The scan rates are 5, 10, 20, 30, and 40 mV/s. (b) Plots of anodic and cathodic peak currents from part a vs the scan rate.

Over the past few decades, experiments have been carried out on carbon-based catalysts. It is, therefore, important to study the electrocatalytic activity of the obtained carbon nanotubes. It is known that ruthenium catalyses many reactions such as the Fishcher−Tropsch synthesis,[52] water−gas shift reaction,[53] ammonia synthesis,[54] the Kobel−Engelhardt reaction,[55] and the hydrogenation of benzene.[56] We, therefore, investigated the electrocatalytic activity of prepared carbon nanotubes for the electroreduction of oxygen. It is worth studying this reaction on carbon nanotubes because it has great technological importance for H_2-O_2 fuel cells. We have carried out preliminary electrocatalytic activity studies of bamboo-shaped CNTs for oxygen reduction reaction. The electrocatalytic test was performed in an acidic aqueous media. The electrolyte was first degassed by bubbling argon for 30 min, after which the background current was recorded. Figure 9 shows the linear sweep voltammogram (LSV) in the absence of oxygen and in the presence of oxygen in a 1M H_2SO_4 solution. The electrocatalytic effect of a Ru-encapsulated carbon-nanotube electrode to O_2 reduction can be clearly observed in the LSVs. This is reflected by two important catalytic features: a significant positive shift of the O_2 reduction potential and a concurrent increase in the oxygen reduction peak current. These are the two important features of any catalysts in fuel cells. The onset potential for oxygen reduction is shifted positively when

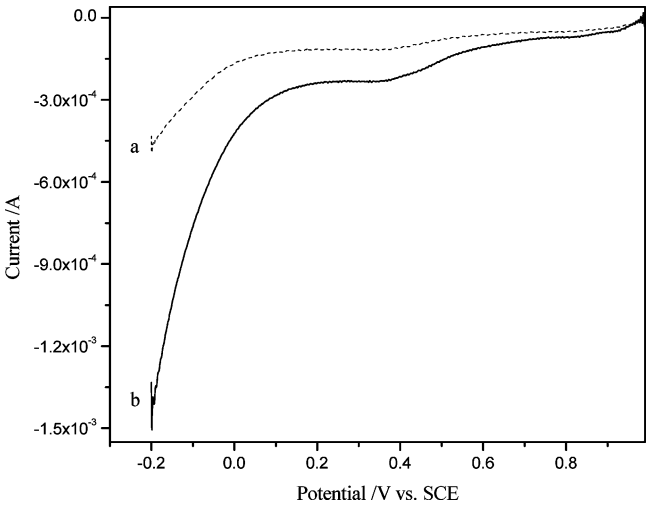

Figure 9. Linear sweep voltammetric response of bamboo-shaped carbon nanotubes: (a) 1 M sulfuric acid; (b) 1M sulfuric acid saturated with oxygen. The scan rate is 10 mV/s.

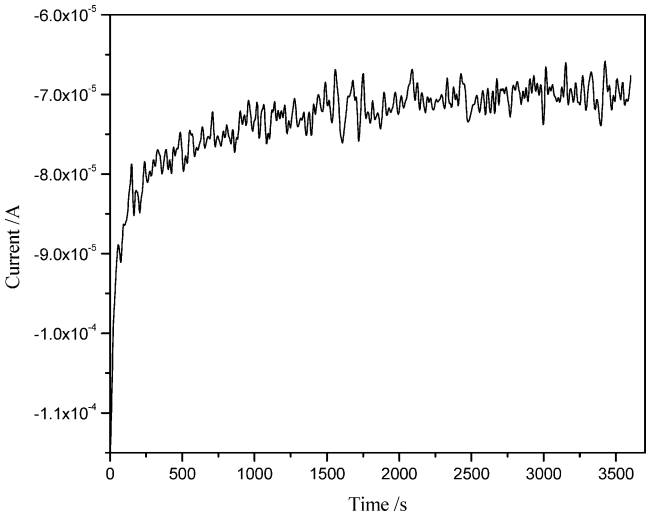

Figure 10. Chronoamperometic response of bamboo-shaped carbon nanotube electrode in 1 M sulfuric acid with continuous bubbling of oxygen. The polarization potential is 0 vs SCE.

compared to the hemin-functionalized MWCNTs,[57] nanosized Au particles immobilized on self-assembled monolayers (SAMs) of cystamine (CYST) and 1,4-benzenedimethanethiol (BDMT),[58] and GC modified with a dicobalt diphorphyrin complex.[59] Figure 10 shows the chronoamperometric response of a bamboo-shaped CNT/GC electrode for oxygen reduction in 1 M sulfuric acid. The electrode was polarized at a potential of 0 V with continuous bubbling of oxygen. It is clear from Figure 10 that the electrode has a high stability for oxygen reduction during the period of investigation.

Conclusions

We have presented a simple and efficient solid-state route for the generation of hydrophilic carbon nanotubes. The prepared carbon nanotubes mostly consist of bamboo-shaped compartments. The generated carbon nanotubes contain surface oxygen functional groups which are evidenced from TGA, IR, XPS, and CV spectroscopic analysis. The electrochemical studies showed the presence of a redox pair in an aqueous acid solution. The presence of disorder in the graphitic carbon and the exposed edge-plane defects in the generated carbon nanotubes are evidenced by Raman studies. A potential application of syn-

thesized carbon nanotubes for oxygen reduction reaction is presented. The high stability of the electrode for oxygen reduction is attributed to the presence of disorder on graphitic carbon nanotubes.

Acknowledgment. The authors thank Dr. Yudith Grinblat and Dr. Tova Tamari for the HRTEM and TEM analyses and Dr. Y. Gofer for the XPS analysis.

Supporting Information Available: TGA and XRD analyses and HRTEM image of bamboo-shaped carbon nanotubes. This material is available free of charge via the Internet at http://pubs.acs.org.

References and Notes

(1) Baughman, R. H.; Zakhidov, A. A.; de Heer. W. A. *Science* **2002**, *297*, 787. Rao, C. N. R.; Satishkumar, B. C.; Govindaraj, A.; Nath, M. *Chem. Phys. Chem.* **2001**, *2*, 78.
(2) Iijima, S. *Nature (London)* **1991**, *354*, 56.
(3) Bethune, D. S.; Kiang, C. H.; deVries, M. S.; Gorman, G.; Savoy, R.; Vazquez, J.; Beyers, R. *Nature (London)* **1993**, *363*, 605.
(4) Journet, C.; Maser, W. K.; Bernier, P.; Loiseau, A.; Lamy de la Chapelle, M.; Lefrant, S.; Denaiard, P.; Lee, R.; Fischer, J. E. *Nature (London)* **1997**, *388*, 756.
(5) Thess, A.; Lee, R.; Nikolaev, P.; Dai, H,; Petit, P.; Robert, J.; Xu, C.; Lee, Y. J.; Fisher, J. E., Smalley, R. E. *Science* **1996**, *273*, 483.
(6) Li, W. Z.; Xie, S. S.; Qain, L. X.; Chang, B. H.; Zou, B. S.; Zhou, W. Y.; Zhao, R. A.; Wang. G. *Science* **1996**, *274*, 1701. Fan, S.; Chapline, M. G.; Franklin, N. R.; Tombler, T. W.; Cassell, A. M.; Dai, H. *Science* **1999**, *283*, 512.
(7) Qin, L. C. *J. Mater. Sci. Lett.* **1997**, *16*, 457.
(8) Hou, H.; Jun, Z.; Weller, F.; Greiner, A. *Chem. Mater.* **2003**, *15*, 3170. Lyu, S. C.; Liu, B. C.; Lee. S. H.; Park, C. Y.; Kang. H. K.; Yang, C.-W.; Lee, C. J. *J. Phys. Chem. B* **2004**, *108*, 2192.
(9) Iyer, V. S.; Vollhardt, K.; Peter. C.; Wilhelm, R. *Angew. Chem., Int. Ed.* **2003**, *42*, 4379.
(10) Wu, J.; Hamaoui, B. E.; Li, J.; Zhi, L.; Kolb, U.; Mullen, K. *Small* **2005**, *1*, 210.
(11) Saito, Y. *Carbon* **1995**, *33*, 979.
(12) Adveena, L. B.; Goncharova, O. V.; Kochubery, D. I.; Zaikovskii, V. I.; Plyasova, L. M.; Vovgorodov, B. N.; Shaikhutdinov, S. K.; *Appl. Catal., A* **1996**, *141*, 117.
(13) Kiselev, N. A.; Sloan, J.; Zakharov, D. N.; Kukivitskii, E. F.; Hutchison, J. L.; Hammer, J.; Kotosonov, A. S. *Carbon* **1998**, *36*, 1149.
(14) Che, G.; Lakshmi, B. B.; Fisher E. R.; Martin, C. R. *Nature* **1998**, *393*, 346. Carmo, M.; Paganin, V. A.; Rosolen, J. M.; Gonzalez, E. R. *J. Power Sources* **2005**, *142*, 169. Chambers, A.; Nemes, T.; Rodriguez, N. M.; Baker, R. T. K. *J. Phys. Chem. B* **1998**, *102*, 2251. Pham-Huu, C.; Keller, N.; Ehret, G.; Ledoux, M. J.; Charbonnière, L.; Ziessel, R. *J. Mol. Catal. A: Chem.* **2001**, *170*, 155.
(15) Hiura, H.; Ebbesen, T. W.; Tanigaki, K. *Adv. Mater.* **1995**, *7*, 275.
(16) Liu, J.; Rinzler, A. G.; Dai, H.; Hafner, J. H.; Bradley, R. K.; Bourl, P. J.; Lu, A.; Iverson, T.; Shelimov, K.; Huffman, C. B.; Fodriguez-Macias, F.; Shon, Y.-S.; Lee, R. R.; Colbert, D. T.; Smalley, R. E. *Science* **1998**, *280*, 1253.
(17) Shaffer, M. S. P.; Faw, X.; Windle, A. H. *Carbon* **1998**, *36*, 1603.
(18) Ago, H.; Kugler, T.; Cacialli, F.; Salaneck, W. R.; Shaffer, M. S. P.; Windle, A. H.; Friend, R. H. *J. Phys. Chem. B* **1999**, *103*, 8116.
(19) Mawhinney, D. B.; Naumenko, V.; Kuznetsova, A.; Yates, J. T.; Liu, J.; Smalley, R. E. *Chem. Phys. Lett.* **2000**, *324*, 213.
(20) Maldonado, S.; Stevenson, K. J. *J. Phys. Chem. B* **2004**, *108*, 11375.
(21) Musameh, M.; Lawrence, N. S.; Wang, J. *Electrochem. Commun.* **2005**, *7*, 14.
(22) Rice, R. J.; McCreery, R. L. *Anal. Chem.* **1989**, *61*, 1637. Goss, C. A.; Brumfield, J. C.; Irene, E. A.; Murray, R. W. *Anal. Chem.* **1993**, *65*, 1378.
(23) Wang, Y. *J. Am. Chem. Soc.* **1994**, *116*, 397.
(24) Liu, S.; Yue, J.; Wehmschulte, R. J. *Nano Lett.* **2002**, *2*, 1439.
(25) Geng, J.; Jefferson, D.; Johnson, B. F. G. *J. Mater. Chem.* **2005**, *15*, 844.
(26) Fan, S.; Chapline, M. G.; Franklin, N. R.; Tombler, T. W.; Casell, A. M.; Dai, H. *Science* **1999**, *283*, 512.
(27) Bethune, D. S.; Klang, C. H.; De Vries, M. S.; Gorman, G.; Savoy, R.; Vasquez, J.; Beyers, R. *Nature* **1993**, *363*, 305.
(28) Ren, Z. F.; Huang, Z. P.; Xu, J. W.; Wang, J. H.; Bush, P.; Siegal, M. P.; Provencio, P. N. *Science* **1998**, *282*, 1105.
(29) Wal, R. L. V.; Ticich, T. M. Curtis, V. E. *Carbon* **2001**, *39*, 2277.
(30) Dai, H.; Rinzler, A. G.; Nikolaev, P.; Thess, A.; Colbert, D. T.; Smalley, R. E. *Chem. Phys. Lett.* **1996**, *260*, 471.
(31) Zhang, Y.; Zhang, H.-B.; Lin, G.-D.; Chen, P.; Yuan, Y.-Z.; Tsai, K. R. *Appl. Catal., A* **1999**, *187*, 213.
(32) Anderson, M.; Alberius-Henning, P.; Jansson, K.; Nygren, M. *J. Mater. Res.* **2000**, *15*, 1822.
(33) Cao, A.; Ci, L.; Li, D.; Wei, B.; Xu, C.; Liang, J.; Wu, D. *Chem. Phys. Lett.* **2001**, *335*, 150.
(34) Mabudafhasi, M. L.; Bodkin, R.; Nicolaides, C. P.; Liu, X.-Y.; Witcomb, M. J.; Coville, N. J. *Carbon* **2002**, *40*, 2737.
(35) Dickcy, E. C.; Grimer, C. A.; Jain, M. K.; Ong, K. G.; Qian, D.; Kichambare, P. D.; Andrews, R.; Jacques, D. *Appl. Phys. Lett.* **2001**, *79*, 4022.
(36) Li, H.; Wang, X.; Liu, Y.; Li, Q.; Jiang, L.; Zhu, D. *Angew. Chem., Int. Ed.* **2001**, *40*, 1743.
(37) Yu, M. F.; Dyer, M. J.; Chen, J.; Qian, D.; Liu, W. K.; Ruoff, R. S. *Phys. Rev. B* **2001**, *64*, 241403.
(38) Lee, C. J.; Park, J. *Appl. Phys. Lett.* **2000**, *77*, 3397. Katayama, T.; Araki, H.; Yoshino, K. *J. Appl. Phys.* **2002**, *91*, 6675.
(39) Reznik, D.; Olk, C. H.; Neumann, D. A.; Copley, J. R. D. *Phys. Rev. B* **1995**, *52*, 116.
(40) Boehm, H. P. *Carbon* **2002**, *40*, 145.
(41) Boehm, H. P.; Diehl, E.; Heck, W.; Sappok, R. *Angew. Chem., Int. Ed.* **1964**, *3*, 669.
(42) Banks, C. E.; Davies, T. J.; Wildgoose, G. G.; Compton, R. G. *Chem. Commun.* **2005**, 829.
(43) Ros, T. G.; vanDillen, A. J.; Geus, J. W.; Koningsbereger, D. C. *Chem.—Eur. J.* **2002**, *8*, 1151.
(44) Ago, H.; Kugler, T.; Cacialli, F.; Salanceck, W. R.; Shaffer, M. S. P.; Windle, A. H.; Friend, R. H. *J. Phys. Chem. B* **1999**, *103*, 8116.
(45) Esumi, K.; Ishigmi, M.; Nakajima, A.; Sawada, K.; Honda, H. *Carbon* **1996**, *34*, 279.
(46) Li, J.; Cassel, A.; Delzeit, L.; Haw, J.; Meyyappan, M. *J. Phys. Chem. B* **2002**, *106*, 888.
(47) Campbell, J. K.; Sun, L.; Crooks, R. M. *J. Am. Chem. Soc.* **1999**, *121*, 3779.
(48) Barisci, J. N.; Wallace, G. G.; Baughmann, R. *J. Electroanal. Chem.* **2000**, *488*, 92.
(49) Ye, J. S.; Liu, X.; Cui, H. F.; Zhang, W. D.; Sheu, F. S.; Lim, T. M. *Electrochem. Commun.* **2005**, *7*, 249.
(50) Kaempgen, M.; Roth, S. *Synth. Met.* **2005**, *152*, 353.
(51) Bard, A. J.; Faulkner, L. R. *Electrochemical Methods*, 2nd ed.; John Wiley & Sons: New York, 2001.
(52) Vannice, M. A. *J. Catal.* **1975**, *37*, 449.
(53) Verdonck, J. J.; Jacobs, P. A.; Vytterhoeven, J. B.; *J. Chem. Soc., Chem. Commun.* **1979**, 181.
(54) Urabe, K.; Shiraton, K.; Ozaki, A. *J. Catal.* **1981**. *72*, 1.
(55) Gustafson, G. L.; Lunsford, J. H. *J. Catal.* **1982**, *74*, 642.
(56) Sun, Z.; Liu, Z.; Han, B.; Wang, Y.; Du, J.; Xie, Z.; Han, G. *Adv. Mater.* **2005**, *17*, 928.
(57) Ye, J. S.; Wen, Y.; Zhang, W. D.; Cui, H. F.; Gan, L. M.; Xu, G. Q.; Sheu, F. S. *J. Electroanal. Chem.* **2004**, *562*, 241.
(58) Raj, C. R.; Abdelrahman, A. I.; Ohsaka, T. *Electrochem. Commun.* **2005**, *7*, 884.
(59) Lu, W. B.; Wang, C. X.; Lv. Q. Y.; Zhou, X. H. *J. Electroanal. Chem.* **2003**, *558*, 59.